International Journal of Engineering Inventions
e-ISSN: 2278-7461, p-ISSN: 2319-6491
Volume 15, Issue 3 [March 2026] PP: 164-173

Scientific Verification of the Appropriateness of the Name "Archimedean Spiral Wind Blade" Based on Projection Method

Jianqiang Wang, Xiaoxu Li, Xuelian Yu, Jiahao Wang, Yuntao Wei, Jixuan Wang, Yonghui Chen, Yingnan Kan
School of Mechanical and Vehicle Engineering, Changchun University, Changchun, CHINA
Corresponding Author: Yingnan Kan

ABSTRACT: *Archimedean Spiral Wind Blades (ASWB) are a novel type of wind turbine blade whose name clearly suggests a geometric relationship with the Archimedean spiral. However, the existing literature lacks a rigorous quantitative verification of this relationship. In this study, based on the original design concept, a standard three-dimensional model of the ASWB was established in SolidWorks, and the spatial boundary curve of the blade was projected onto a plane. The resulting projection curve was then compared with a two-dimensional Archimedean spiral generated from its analytical equation. Through geometric comparison, discrete-point analysis, and evaluation of the linear relationship between polar radius and polar angle, it was demonstrated that the projection curve satisfies the defining equation of the Archimedean spiral, $r=a+b\theta$. The maximum radial deviation between the two curves was 0.0909 mm, and the average deviation was 0.0108 mm, both of which are far below the typical range of engineering tolerances. Linear regression analysis further showed a strong linear relationship between the polar radius and the polar angle, with the coefficient of determination approaching 1. These results indicate that the projected boundary curve of the ASWB is consistent with the Archimedean spiral, thereby providing a clear scientific explanation for the name "Archimedean Spiral Wind Blade."*

Key words: *Archimedean Spiral Wind Blade; Projection method; Geometric verification; Linear regression*

Date of Submission: 15-03-2026 Date of acceptance: 31-03-2026

I. INTRODUCTION

The Archimedean Spiral Wind Blade (ASWB) is a novel type of wind blade proposed in 2006 by the Dutch inventor Rinus Mieremet. The Archimedean Spiral Wind Rotor (ASWR) consists of three ASWBs, and its rotational axis is parallel to both the ground and the wind direction. Therefore, the Archimedean Spiral Wind Turbine (ASWT) belongs to the category of horizontal-axis wind turbines [1–5].

Compared with conventional horizontal-axis wind turbines, the ASWT exhibits many unique characteristics. Although the ASWT mainly operates on drag and is therefore classified as a drag-type wind turbine [5–17], a large number of experimental and numerical studies have shown that its tip-speed ratio can exceed 1, with the highest reported value reaching 4.0, which is a clear distinction between the ASWT and traditional drag-type wind turbines [18]. In terms of performance, the maximum power coefficient of the ASWT has been reported to reach 51.17% [19], indicating strong potential for energy capture. Even more uniquely, due to the special aerodynamic shape of its spiral rotor, the ASWT can automatically align itself with the incoming wind without the need for an external yaw system [15]. This challenges the traditional understanding that horizontal-axis wind turbines must be equipped with a yaw system [1][2][3][5][8].

However, since the advent of the ASWB, its development has shown a trend in which commercialization has advanced ahead of theoretical research. Existing studies have mostly focused on its aerodynamic performance [15–22], while fundamental theoretical investigations remain relatively scarce. One essential question still lacks a detailed and scientifically grounded explanation: why is this blade named after the "Archimedean spiral"? At present, only two reasons have been provided by the inventor. First, the blade was named in tribute to the ancient Greek mathematician Archimedes, because its invention was inspired by his approach to geometric research. Second, the formation process of the blade surface is closely related to the two-dimensional Archimedean spiral in a plane. However, although the inventor provided relevant schematic illustrations, the corresponding explanation remains brief and qualitative, without presenting a specific geometric model or mathematical formulation.

Apart from the qualitative explanation provided by the inventor, no published literature has yet been found to seriously investigate the rationale behind the naming of this blade. Although the name is highly effective from the perspectives of product promotion and market expansion, in the long run, any novel blade lacking a solid

theoretical foundation will find it difficult to compete sustainably with conventional wind turbine blades that are supported by extensive theoretical research. As noted earlier, theoretical studies on the ASWB remain relatively limited. Therefore, if this blade is to receive sustained support at the theoretical level, the first issue that should be addressed is whether its naming is academically justified.

If the Archimedean Spiral Wind Blade had been named after its inventor, there would be no need to examine the rationality of its name in depth. In reality, however, the name "Archimedean Spiral Wind Blade" strongly suggests a relationship between the blade and the Archimedean spiral, while at the same time no literature can currently be found that investigates this relationship from a scientific perspective. Therefore, demonstrating the rationality of the name of this novel blade naturally becomes the first issue to be addressed in the study of its fundamental theory.

In view of the above situation, this paper first proposes the core hypothesis that the projection of the boundary curve of the ASWB onto a specific plane is a strictly two-dimensional Archimedean spiral. To verify this hypothesis, this study intends to employ several engineering software tools and, in combination with a standardized geometric model and mathematical formulas, compare the projection of the boundary curve of the ASWB with a true two-dimensional Archimedean spiral. If the two are identical, then this paper will, from a scientific perspective, demonstrate the rationality of the name ASWB, so that the term ASWB will no longer be merely a vague product name, but will instead become a serious object of scientific research. The technical roadmap is shown in Figure 1.

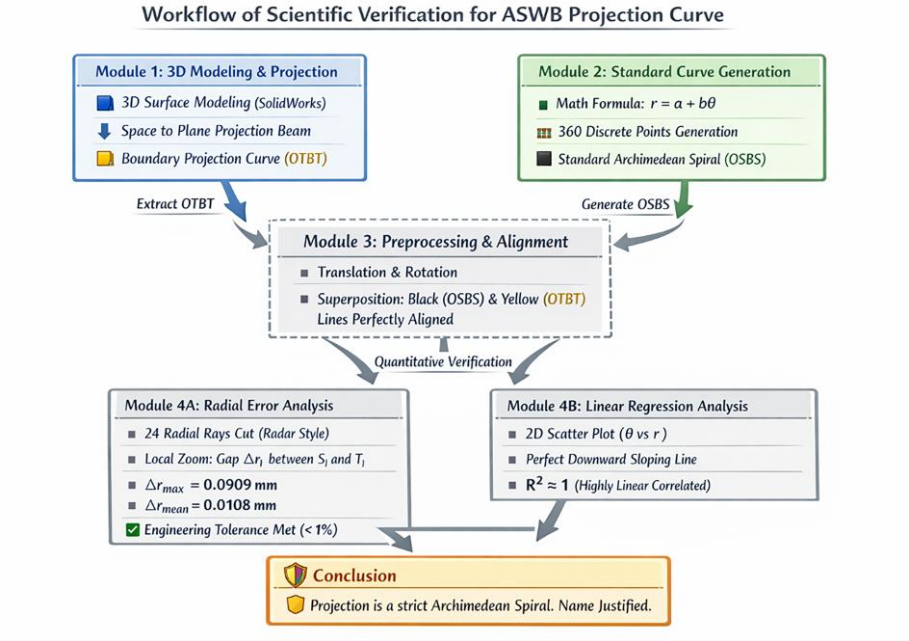

Fig. 1 Technical Roadmap

II. Theoretical Foundation

Original Explanation of the Formation Mechanism of the ASWB Surface

Regarding the generation principle of the ASWB surface, the inventor's original statement can be roughly translated as follows: "An Archimedean rotor blade is an elongated plane. By stretching it along the depth direction (that is, the direction perpendicular to the plane), the plane acquires volume. On a sheet of paper, cut out the shape enclosed between an arc with radius R and a planar spiral curve; then rotate and simultaneously stretch this shape, and the spatial form of the Archimedean rotor blade can be obtained." As shown in Figures 2 and 3 [23].

Reference [23] states that the ancient Greek scholar Archimedes, in his study of geometry, often stretched and rotated straight lines (or curves) on a plane simultaneously, thereby creating spatial surfaces (or volumes). The creation of the ASWB was inspired by this geometric research approach of Archimedes. Therefore, the blade was named the "Archimedean Spiral Wind Blade" to express the inventor's respect for the ancient Greek scholar Archimedes.

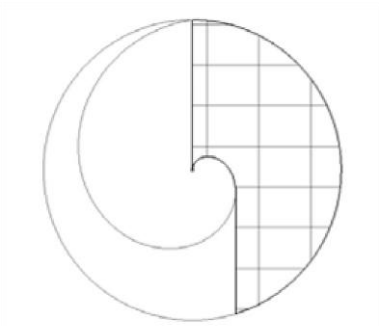

Fig 2. Closed Plane Figure Before Deformation

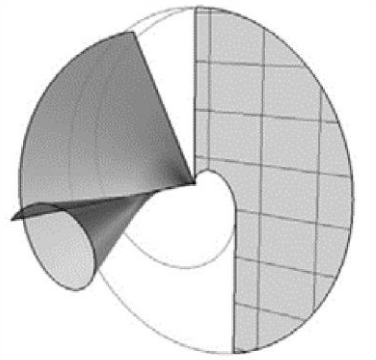

Fig 3. Archimedean Spiral Surface After Deformation

Definition of the Archimedean Spiral

In the plane *xOy*, when a point *P* moves along the rotating ray *OP* at a constant speed *v*, while *OP* simultaneously rotates about point *O* with a constant angular velocity ω, the trajectory of point *P* is called an Archimedean spiral, as shown in Figure 4.

In Figure 4, taking time *t* as the independent variable, assume that point *P* starts from point *O* at time t=0, and that at t=0, the instantaneous velocity of point *P* is along the positive direction of the *y*-axis. Let the rotation direction of ray *OP* be clockwise, with angular speed ω (ω>0). Suppose that at time *t*, the angle between ray *OP* and the *y*-axis is denoted by θ, and the length of *OP* is denoted by *r*. Then, in polar coordinates, the coordinates of point *P*, that is, the equation of the Archimedean spiral, can be written as:

$$r = b \times \theta, \quad -2\pi \le \theta \le 0 \tag{1}$$

In Eq. (1), r=vt, and *b* is an undetermined constant. In this paper, for consistency with the original description (see Figure 3), the ray *OP* is assumed to rotate clockwise. Meanwhile, considering that the counterclockwise direction is generally taken as the positive direction, after time *t*, the angle between ray *OP* and the *y*-axis is: θ=ωt.

For the convenience of describing Figure 4, it is specified that when the angle between ray *OP* and the *y-axis* is exactly θ=2π, the length of *OP* is exactly *R*. Substituting this assumption into Eq. (1) yields the following equation:

$$R = b \times (-2\pi) \tag{2}$$

From Eq. (2), the expression for *b* can be obtained as:

$$b = -\frac{R}{2\pi} \tag{3}$$

Thus, the coordinates of point *P*, that is, the equation of the Archimedean spiral in the polar coordinate system, can be written as:

$$r = -\frac{R}{2\pi} \times \theta, \quad -2\pi \le \theta \le 0 \tag{4}$$

By converting the polar coordinates of point *P* into Cartesian coordinates, the equation of the Archimedean spiral in the Cartesian coordinate system can be written as:

$$\begin{cases} x = r\cos\theta = -\dfrac{R}{2\pi}\theta\cos\theta \\ y = r\sin\theta = -\dfrac{R}{2\pi}\theta\sin\theta \end{cases} \tag{5}$$

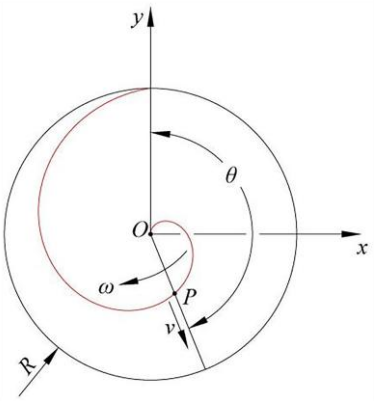

Fig 4. Definition of the Archimedean Spiral in a Plane

3D Modeling of the Archimedean Spiral Surface

At present, the establishment of the standard ASWB model in most published studies and online resources is based on the SolidWorks modeling process. To establish a standard geometric model of the ASWB, this study constructed a three-dimensional surface using SolidWorks according to its design principle. The key steps are as follows:

1) Sketch drawing: First, establish a three-dimensional Cartesian coordinate system *XYZ*, in which the *X*-axis, *Y*-axis, and *Z*-axis are mutually perpendicular. The *XY* plane is parallel to the plane of the paper, and the *Z*-axis is perpendicular to the plane of the paper. The initial sketch is then drawn on the *XY* reference plane, as shown in Figure 5. A solid line segment *AB* is defined, and the auxiliary dashed segments *OA* and *OB* are constructed in relation to it. Here, *OA* is in the horizontal direction, *OB* (in this paper, *OB*=75 mm is used as an example) is perpendicular to *OA*, and $\angle BAO$=60°.

2) Definition of the spatial helix: In the *YZ* reference plane, a base circle is drawn with point *O* as the center and *OB* as the radius. Using this circle as a reference, a spatial spiral curve is defined with its starting point at *B* and its end point at *C*; therefore, it is denoted as spiral *BC*. The parameters of spiral *BC* are configured as follows: the radius decreases linearly from 75 mm to 0, the pitch remains constant at 75 mm, the number of revolutions is exactly one, and the rotation direction is counterclockwise. Due to the software limitations of SolidWorks, to approximate the theoretical apex *C* (which is located on the *OX* axis), the radius of the top circle is set to 0.05 mm. This minimizes the distance between point *C* and the axis, thereby ensuring modeling precision, as illustrated in Fig. 6 and Fig. 7.

3) Surface generation: Using the Boundary Surface feature in SolidWorks, the initial sketch (Figure 5), line segment *OC*, spatial helix *BC*, and auxiliary dashed segment *OA* are selected in sequence to generate the so-called Archimedean spiral surface. The resulting surface model and its three-view drawings are shown in Figure 8.

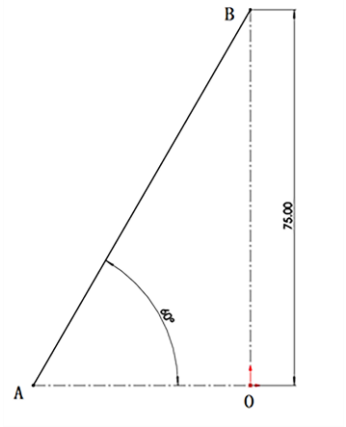

Fig 5. Sketch on the XY Plane

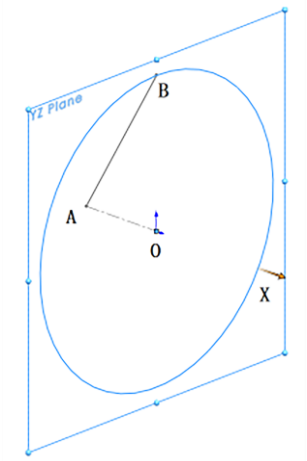

Fig 6. Definition of the Base Circle of the Spatial Helix

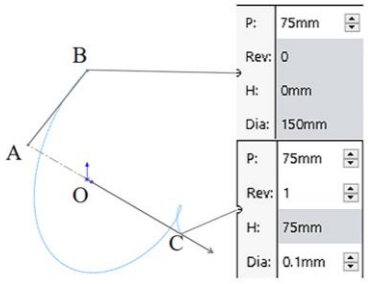

Fig 7. Definition of the Parameters of the Spatial Helix

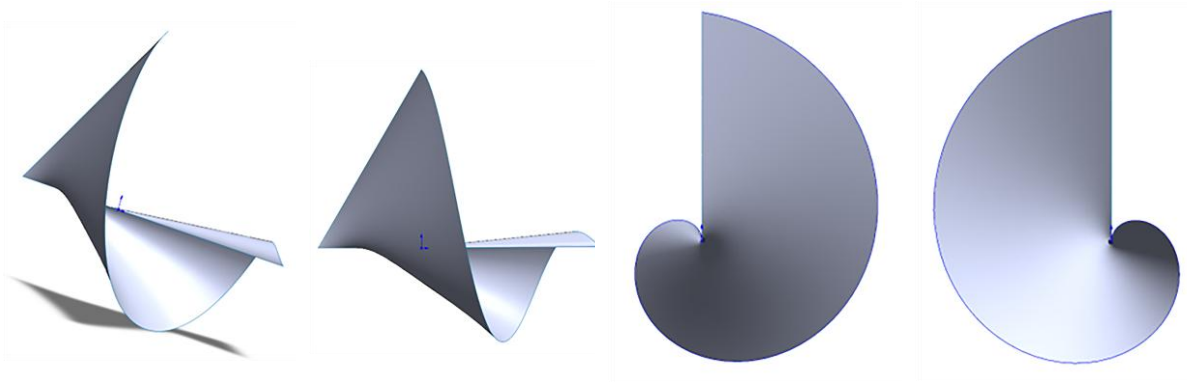

(a) Isometric View **(b) Front View** **(c) Left View** **(d) Right View**

Fig 8. Archimedean Spiral Surface

III. Generation of the Standard Archimedean Spiral and the projection of boundary curve

The equation of the standard Archimedean spiral in the Cartesian coordinate system is given by Eq. (5), and the drawing process is as follows:

Using MATLAB and based on Eq. (5), let R=75, and within the defined domain take (θ1=1°, θ2=2°, …, θ360=360°). Then, calculate the Cartesian coordinates of 360 discrete points:($x_{\theta 1}$,$y_{\theta 1}$),($x_{\theta 2}$,$y_{\theta 2}$),…,($x_{\theta 360}$,$y_{\theta 360}$), and export the coordinate data for further processing and save it as a script file. Subsequently, in AutoCAD, the coordinate file is read through the script command. Based on the "pline" command and the coordinate data of the discrete points in the file, AutoCAD plots a series of coordinate points and connects them sequentially with straight-line segments, thereby generating the standard Archimedean spiral O_SB_S, as shown in Figure 9. Its starting point is denoted by O_S, and its ending point is denoted by B_S.

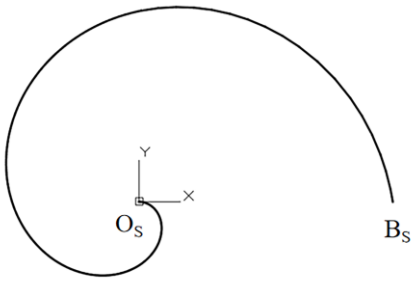

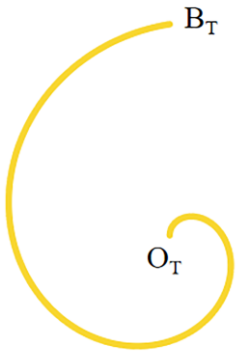

Fig 9. Standard Archimedean Spiral O_SB_S **Fig 10. Projection Curve O_TB_T**

Obtaining the projection of the boundary curve of the ASWB

Using the "Make Drawing from Part/Assembly" function in SolidWorks, the projection of the ASWB surface model generated in Section 1.3 onto the *YZ* plane is obtained, as shown in Figure 10. The projected curve is denoted as O_TB_T, with O_T as its starting point and B_T as its ending point. Figure 10 is then saved in DWG format for subsequent use in AutoCAD.

IV. Mathematical Validation of the Projection Curve

Proposed Hypothesis and Verification Strategy

It is worth noting that, from Figure 8, the projection of the boundary curve of the ASWB (namely, the helix *BC*) onto the *YZ* plane (see Figure 6) can be clearly observed, and this projection (as shown in Figure 10) is visually highly similar to the standard Archimedean spiral in a plane. In fact, almost everyone assumes that this projection is exactly the standard Archimedean spiral in a plane; in other words, that the projection of the spatial helix *BC* defined in Section 1.3 onto the *YZ* plane is an Archimedean spiral, or equivalently, that the spatial helix *BC* is a three-dimensional Archimedean spiral in the mathematical sense. However, this view has never been rigorously proven. This paper argues that proving this fact is of great importance for the subsequent theoretical study of the ASWB.

Based on the above discussion and in conjunction with the Introduction, this paper proposes the following specific hypothesis: the projection curve O_TB_T and the standard two-dimensional Archimedean spiral O_SB_S are mathematically identical curves.

Geometric Pre-processing Prior to Quantitative Verification

The projection curve O_TB_T and the standard Archimedean spiral O_SB_S were imported into the same AutoCAD file, as shown in Figure 11(a). The black curve represents the standard Archimedean spiral O_SB_S (noting that O_SB_S is oriented horizontally), while the yellow curve represents the projection curve O_TB_T. Keeping the standard curve O_SB_S stationary, the projection curve O_TB_T was translated as a whole to make point O_T coincide with point O_S, as shown in Figure 11(b). Subsequently, the projection curve O_TB_T was rotated to align points B_S and B_T on the same horizontal line, as shown in Figure 11(c).

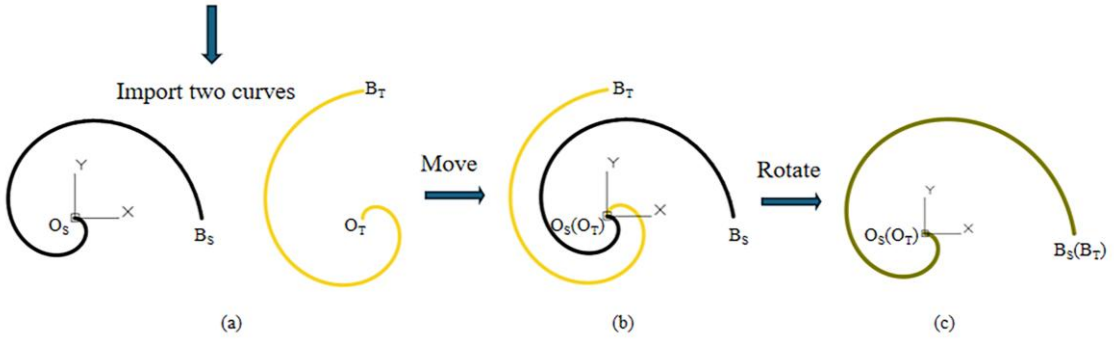

Fig. 11 Comparison and alignment of the two curves

Radial error analysis

To quantitatively evaluate the consistency, 24 rays are drawn starting from the center O_S in Fig. 11(c). Each ray is denoted as L_i (i=1, 2, ..., 24), with an angle of 15° between any two adjacent rays. The angle between L_i and the horizontal line is represented by θ_i, $\theta_i = -(i \times 15)°$, as shown in Fig. 12.

The intersection between L_i and the standard Archimedean spiral O_SB_S is denoted as S_i. In the polar coordinate system, the coordinates of S_i are (r_{Si}, θ_i), and in the Cartesian coordinate system, the coordinates of S_i are (x_{Si}, y_{Si}).

The intersection between L_i and the projection curve O_TB_T is denoted as T_i. In the polar coordinate system, the coordinates of T_i are (r_{Si}, θ_i), and in the Cartesian coordinate system, the coordinates of T_i are (x_{Ti}, y_{Ti}).

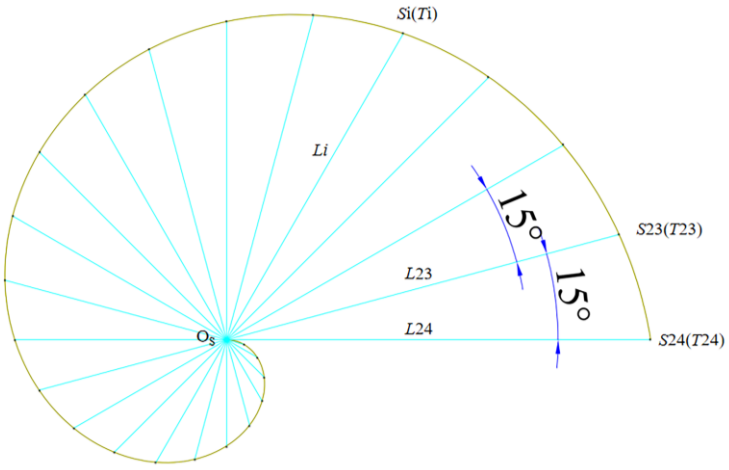

Fig. 12 Ray diagram

Let the distance between O_S and S_i be r_{Si}. According to Equation (4) and setting R=75, the point S_i on the standard curve O_SB_S satisfies Equation (6):

$$x_{Si} = -\frac{75}{2\pi}\theta_i \cos\theta_i$$
$$y_{Si} = -\frac{75}{2\pi}\theta_i \sin\theta_i \quad , \quad -2\pi \le \theta_i \le 0 \tag{6}$$
$$r_{Si} = -\frac{75}{2\pi}\theta_i$$

Calculate the coordinates (x_{Si}, y_{Si}) of S_i according to Equation (6), and compute the corresponding r_{Si}. The calculated data are listed in Table 1.

Let the distance between O_T and T_i be denoted as r_{Ti}. The coordinates (x_{Ti}, y_{Ti}) of T_i are measured in AutoCAD, and the corresponding r_{Ti} are calculated by $r_{Ti} = \sqrt{x_{Ti}^2 + y_{Ti}^2}$. The measured data are presented in Table 1.

Table 1 Discrete point data

θ_i	x_{Si}	y_{Si}	x_{Ti}	y_{Ti}	r_{Si}	r_{Ti}	e_i
0	0.0000	0.0000	0.0000	0.0000	0.0000	0.0000	0.0000
-15	3.0185	-0.8088	3.0179	-0.8087	3.1250	3.1244	0.0006
-30	5.4127	-3.1250	5.4121	-3.1247	6.2500	6.2494	0.0006
-45	6.6291	-6.6291	6.6286	-6.6286	9.3750	9.3743	0.0007
-60	6.2500	-10.8253	6.2496	-10.8247	12.5000	12.4992	0.0008
-75	4.0440	-15.0926	4.0438	-15.0918	15.6250	15.6241	0.0009
-90	0.0000	-18.7500	0.0000	-18.7490	18.7500	18.7490	0.0010
-105	-5.6617	-21.1296	-5.6614	-21.1286	21.8750	21.8739	0.0011
-120	-12.5000	-21.6506	-12.4994	-21.6496	25.0000	24.9988	0.0012
-135	-19.8874	-19.8874	-19.8864	-19.8864	28.1250	28.1236	0.0014
-150	-27.0633	-15.6250	-27.0620	-15.6242	31.2500	31.2485	0.0015
-165	-33.2037	-8.8969	-33.2021	-8.8965	34.3750	34.3734	0.0016
-180	-37.5000	0.0000	-37.4983	0.0000	37.5000	37.4983	0.0017
-195	-39.2407	10.5145	-39.2390	10.5141	40.6250	40.6232	0.0018
-210	-37.8886	21.8750	-37.8870	21.8741	43.7500	43.7481	0.0019
-225	-33.1456	33.1456	-33.1443	33.1443	46.8750	46.8731	0.0019
-240	-25.0000	43.3013	-24.9991	43.2996	50.0000	49.9981	0.0019
-255	-13.7498	51.3148	-13.7493	51.3130	53.1250	53.1232	0.0018
-270	0.0000	56.2500	0.0000	56.2482	56.2500	56.2482	0.0018
-285	15.3674	57.3518	15.3589	57.3201	59.3750	59.3421	0.0329
-300	31.2500	54.1266	31.2321	54.0956	62.5000	62.4642	0.0358
-315	46.4039	46.4039	46.3764	46.3764	65.6250	65.5862	0.0388

-330	59.5392	34.3750	59.4605	34.3296	68.7500	68.6591	0.0909
-345	69.4259	18.6026	69.3798	18.5903	71.8750	71.8273	0.0477
-360	75.0000	0.0000	75.0000	0.0000	75.0000	75.0000	0.0000

Assume that the point T_i on the projection curve O_TB_T satisfies the following formula:

$$r_{Ti} = -\frac{75}{2\pi}\theta_i + e_i, \quad -2\pi \le \theta_i \le 0, \quad e_i = r_{Si} - r_{Ti}.$$

Let the maximum deviation between r_{Si} and r_{Ti} be denoted as $\Delta r_{\max} = \max(|e_i|)$, and let the average deviation between r_{Si} and r_{Ti} be denoted as $\Delta r_{avg} = \sum_{i=1}^{25} |e_i| / 25$.

As shown in Table 1, the maximum deviation is $\Delta r_{\max}$ =0.0909 mm, and the average deviation is $\Delta r_{avg} = \sum \Delta r_i / 25$ =0.0108 mm.

In engineering practice, a maximum relative radial deviation of 1%–2% is typically set as the threshold range for the acceptance criterion. The projection curve O_TB_T is considered geometrically equivalent to the standard Archimedean spiral O_SB_S only when the deviations at all sampling points are within this threshold.

To determine the qualification, the relative error rate ε on each ray L_i is calculated as $\varepsilon = |e_i| / r_{Si} \times 100\%$. If the maximum error rate ε is less than the preset threshold, the consistency is deemed qualified. Based on the data in Table 1, $\varepsilon_{\max}$ =0.0122 % is obtained, which falls within the threshold range. Therefore, from an engineering perspective, the projection curve O_TB_T is considered to be highly consistent with the standard Archimedean spiral O_SB_S.

Analysis of the Linear Relationship between Polar Radius and Polar Angle

To prove that the projection curve O_TB_T is identical to the standard Archimedean spiral O_SB_S, i.e., r and θ exhibit a strict linear relationship, a scatter plot is first generated based on the data (θ_i, r_{Ti}) in Table 1, as shown in Figure 13.

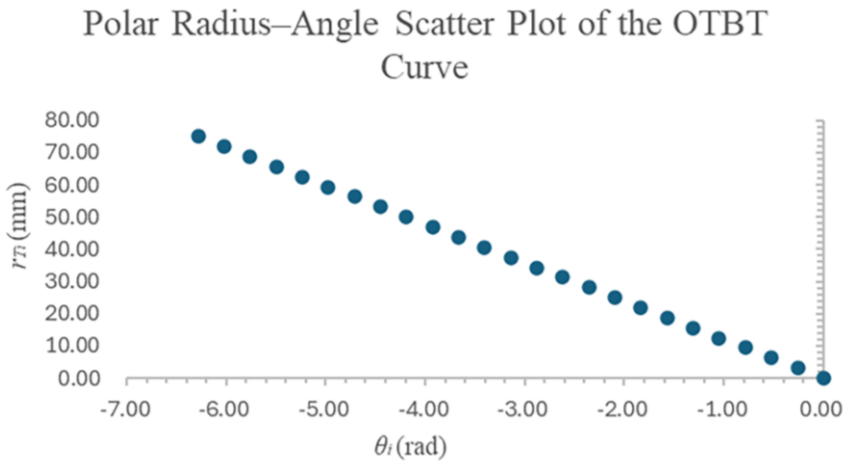

Fig. 13 Polar radius vs. polar angle scatter plot of curve O_TB_T

As observed from Fig. 13, r exhibits a decreasing trend as θ increases, and this relationship is strictly linear. Consequently, a linear regression model is established and expressed as Equation (7), where $\hat{a}_T$ and $\hat{b}_T$ denote the unknown parameters in the model.

$$\hat{r}_T = \hat{a}_T + \hat{b}_T\theta \tag{7}$$

Given that the starting point O_T of the projection curve O_TB_T has been aligned with the starting point O_S

of the standard Archimedean spiral O_SB_S (i.e., r=0 at θ=0), it directly follows from Equation (7) that $\hat{a}_T$ =0.

Using the least squares method, the estimated value of b_T and the coefficient of determination R^2 are calculated based on Equations (8) and (9) and the data in Table 1:

$$\hat{b}_T = \frac{\sum_{i=1}^{n}(\theta_i - \bar{\theta})(r_{Ti} - \bar{r}_T)}{\sum_{i=1}^{n}(\theta_i - \bar{\theta})^2} \tag{8}$$

$$R^2 = \frac{\sum_{i=1}^{n}(\hat{r}_i - \bar{r})^2}{\sum_{i=1}^{n}(r_i - \bar{r})^2} \tag{9}$$

The results obtained are: $\hat{b}_T = -11.9299$, $\hat{r}_T = -11.9299\theta$, and the coefficient of determination R^2=0.99999941≈1.

For the standard Archimedean spiral O_SB_S, the theoretical values of a and b calculated from Equation (4) are and a=0 and b=-75/2π≈-11.9366, respectively. Using the theoretical value as a reference, the relative error of $\hat{b}$ is $(\hat{b} - b)/b \times 100\% = -0.05606\% \approx 0$.

Based on the above calculation results, the relative error of the coefficient b in the regression equations for the two curves is extremely small and negligible, and the coefficient of determination is almost equal to 1, indicating a perfect linear relationship. The corresponding errors are primarily attributed to the precision settings during the software-based curve generation and an insufficient number of sampling points.

V. Conclusion

By establishing a rigorous mathematical projection model and a multidimensional quantitative analysis framework, this paper conducted an in-depth investigation into the geometric boundary characteristics of the Archimedean spiral wind blade (ASWB). The main conclusions are drawn as follows:

1) By innovatively developing a multi-ray (24 rays) radial deviation evaluation model, quantitative analysis reveals that the maximum absolute radial deviation between the projection curve and the standard Archimedean spiral is merely 0.0909 mm, with an average absolute deviation as low as 0.0108 mm. The relative error rate (0.0122％) is significantly lower than the standard acceptance threshold of 1%–2% commonly applied in engineering practice and manufacturing tolerances. This fully demonstrates that the blade curve achieves exceptionally high geometric fidelity at the practical engineering scale.

2) Linear regression analysis was conducted based on the discrete point data in the polar coordinate system. The results indicate that the coefficient of determination (R^2) of the fitted equation for the projection curve is almost equal to 1. Simultaneously, the relative error (-0.05606%) between the calculated regression coefficients and the theoretical reference values is negligible. From the perspective of mathematical statistics and curve fitting, this confirms that the polar radius of the projected curve exhibits a strict uniform linear increment as the polar angle increases.

3) Based on a comprehensive synthesis of the aforementioned geometric projection, deviation quantification, and statistical regression analysis, this paper confirms—through rigorous data and mathematical derivation—that the projection curve of the boundary of ASWB is an authentic Archimedean spiral. This research outcome not only provides a clear and indisputable scientific basis for the naming of the "Archimedean spiral wind blade," thereby filling a theoretical gap characterized by the previous lack of rigorous quantitative verification in this field, but also establishes a crucial geometric foundation for the subsequent aerodynamic performance optimization and high-precision CNC machining of this type of wind blade.

Acknowledgements

We acknowledge the support from the Doctoral Research Start-up Fund of Changchun University (Grant No. 2023JBE01L01).

REFRENCES

[1]. TONG W. Fundamentals of wind energy[M]. Southampton, UK: WIT press, 2010.
[2]. LIU J, LIN H, ZHANG J, et al. Review on the technical perspectives and commercial viability of vertical axis wind turbines[J]. Ocean Engineering, 2019, 182: 608-626.
[3]. SCHUBEL P J, CROSSLEY R J. Wind turbine blade design[J]. Energies, 2012, 5(9): 3425-3449.
[4]. HANSEN M. Aerodynamics of wind turbines[M]. London; New York: Routledge, 2015.
[5]. MANWELL J F, MCGOWAN J G, ROGERS A L, et al. Wind energy explained: theory, design and application[M]. Hoboken: John Wiley & Sons, 2010.
[6]. HEMAMI A. Wind turbine technology[M]. Toronto: Nelson Education, 2011.
[7]. NELSON V. Innovative wind turbines: An illustrated guidebook[M]. Boca Raton: CRC Press, 2019.
[8]. WILSON R E, SPERA D A. Wind Turbine Technology: Fundamental Concepts in Wind Turbine Engineering[J]. ASME, New York, 2009.
[9]. WANG H, XIONG B, ZHANG Z, et al. Small wind turbines and their potential for internet of things applications[J]. IScience, 2023, 26(9).
[10]. TANINO T, YOSHIHARA R, MIYAGUNI T. A, et al. Study on a Casing Consisting of Three Flow Deflectors for Performance Improvement of Cross-Flow Wind Turbine[J]. Energies, 2022, 15(16): 6093.
[11]. KUMAR R, RAAHEMIFAR K, FUNG A S, et al. A critical review of vertical axis wind turbines for urban applications[J]. Renewable and Sustainable Energy Reviews, 2018, 89: 281-291.
[12]. ABRAHAM J P, PLOURDE B D, MOWRY G S, et al. Summary of Savonius wind turbine development and future applications for small-scale power generation[J]. Journal of Renewable and Sustainable Energy, 2012, 4(4).
[13]. TAYEBI A, TORABI F. Flow control techniques to improve the aerodynamic performance of Darrieus vertical axis wind turbines: A critical review[J]. Journal of Wind Engineering and Industrial Aerodynamics, 2024, 252: 105820.
[14]. RUDRAPAL D, ACHARYA S. Characterization of a novel lift-drag-driven air-activated hybrid vertical axis wind turbine[J]. Sustainable Energy Technologies and Assessments, 2023, 59: 103415.
[15]. KIM K C, JI H S, KIM Y K, et al. Experimental and numerical study of the aerodynamic characteristics of an archimedes spiral wind turbine blade[J]. Energies, 2014, 7(12): 7893-7914.
[16]. SAFDARI A, KIM K C. Aerodynamic and structural evaluation of horizontal archimedes spiral wind turbine[J]. Journal of Clean Energy Technologies, 2015, 3(1): 34-38.
[17]. JANG H, Kim D, HWANG Y, et al. Analysis of Archimedes spiral wind turbine performance by simulation and field test[J]. Energies, 2019, 12(24): 4624.
[18]. KIM K C, KIM Y K, JI H S, et al. Aerodynamic characteristics of horizontal axis wind turbine with Archimedes spiral blade[C]//ASME International Mechanical Engineering Congress and Exposition. American Society of Mechanical Engineers, 2013, 56321: V07BT08A070.
[19]. JI H S, BAEK J H, MIEREMET R, et al. The aerodynamic performance study on small wind turbine with 500W class through wind tunnel experiments[J]. International Journal of Renewable Energy Sources, 2016, 1: 7-12.
[20]. EBRAHIMI S, GHASSEMI M A. Numerical aerodynamics analysis of the of the Archimedes screw wind turbine[J]. Int. J Multidisciplinary Sci & Eng, 2018: 12-15.
[21]. HAMID H, ABD EL MAKSOUD R M. A comparative examination of the aerodynamic performance of various seashell-shaped wind turbines[J]. Heliyon, 2023, 9(6).
[22]. LU Q, LI Q, KIM Y K, et al. A study on design and aerodynamic characteristics of a spiral-type wind turbine blade[J]. Journal of the Korean society of visualization, 2012, 10(1): 27-33.
[23]. JI H S, KIM K C, BAEK J H, et al. The aerodynamic method of the Archimedes Windturbine[J]. Journal of Power Solutions, 2014.